

Supplementary material

Atmospheric stratification over Namibia and the southeast Atlantic Ocean

Danitza Klopper^{1,2}, Stuart J. Piketh¹, Roelof Burger¹, Simon Dirkse³ and Paola Formenti⁴

¹North-West University, School for Geo- and Spatial Sciences, Potchefstroom, South Africa

²University of Limpopo, Department of Geography and Environmental Studies, Polokwane, South Africa

³ Namibia Meteorology Service, Windhoek, Namibia

⁴ Université de Paris and Univ Paris Est Creteil, CNRS, LISA, F-75013 Paris, France

Correspondence to: Stuart John Piketh (stuart.piketh@nwu.ac.za)

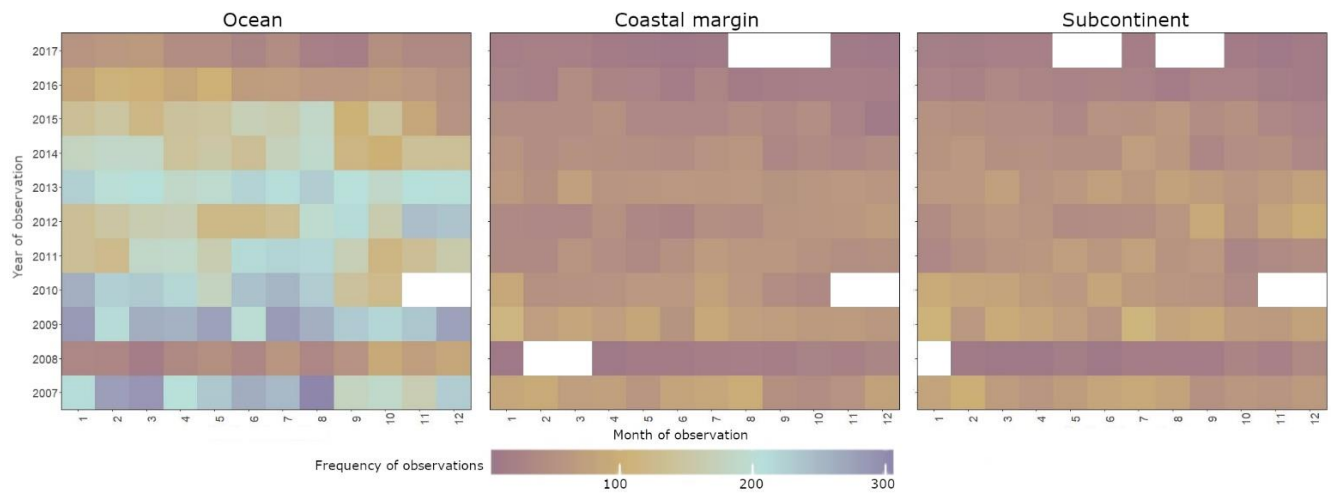


Figure S.1: Frequency of COSMIC GPS-RO measurements by month and year made over the ocean, coastal margin and subcontinent. Blank cells indicate months with less than 10 measurements within the region of interest and therefore excluded from further analysis.

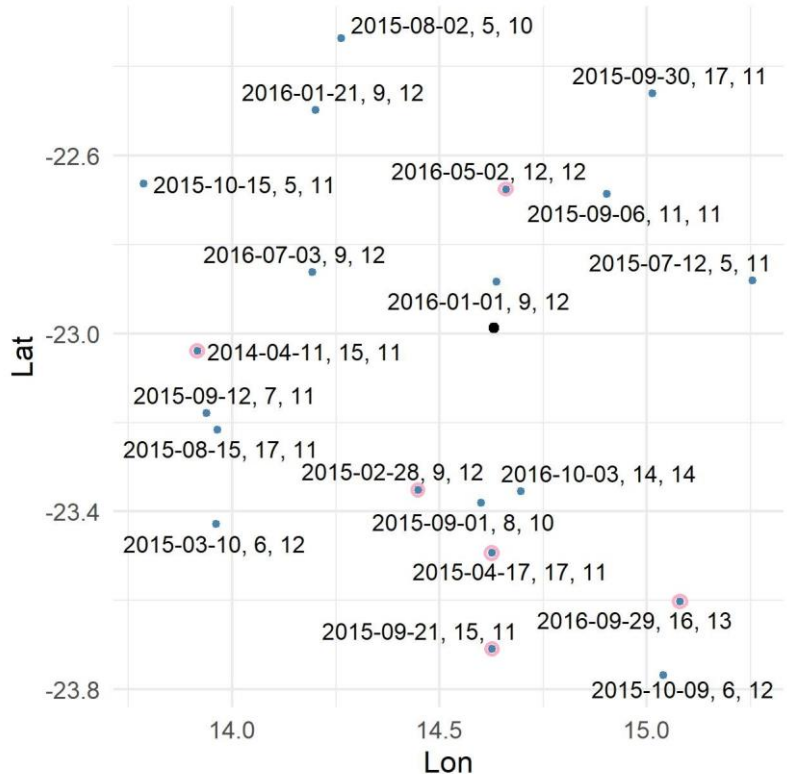


Figure S.2: The location of GPS-RO measurements co-located within 100 km and 6 hours of Walvis Bay (location indicated by the black dot) radiosonde release. Those points circled in pink indicate those points where differences in heights estimated by the MG method for the two datasets, was greater than 1000 m.

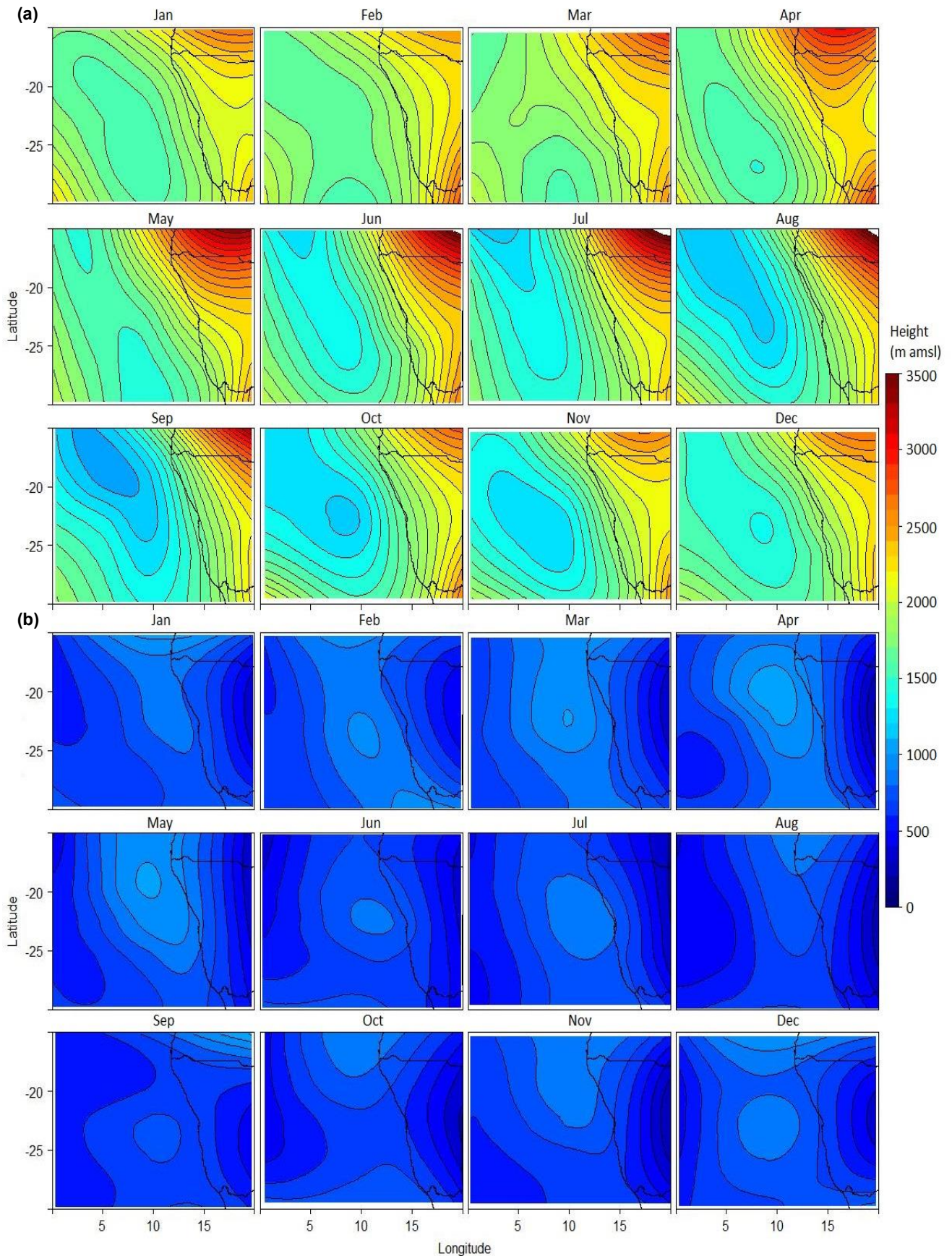


Figure S.3: The monthly (a) mean and (b) standard deviation of the height of the MG of refractivity over the area of interest. Polynomial smoothing was applied to the data.

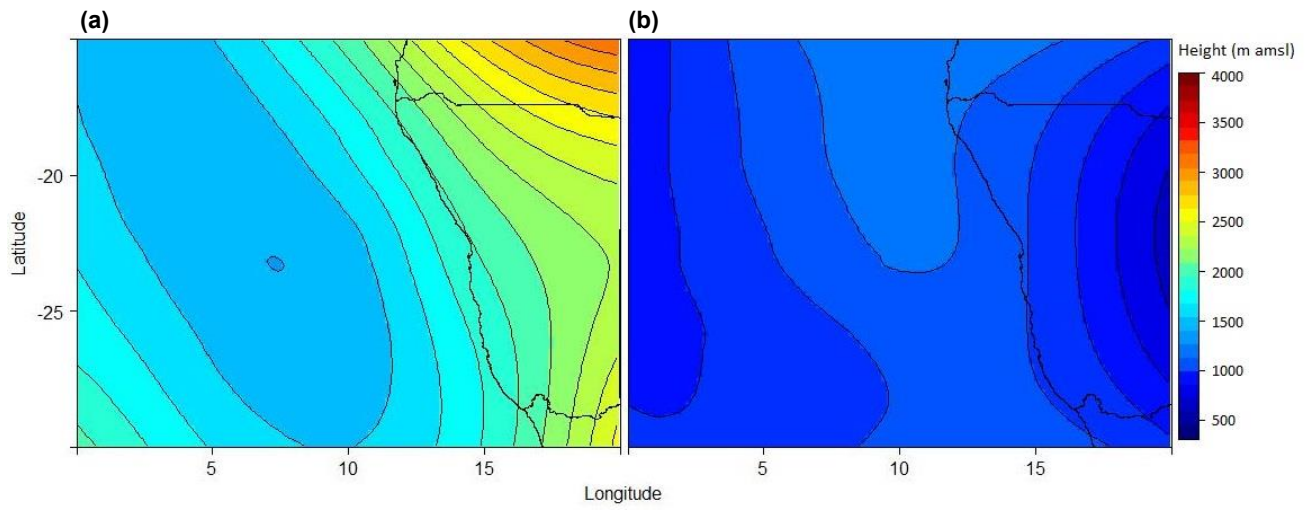


Figure S.4: The overall (a) mean and (b) standard deviation of the height of the MG of refractivity over the area of interest between 2007 and 2017. Polynomial smoothing was applied to the data.

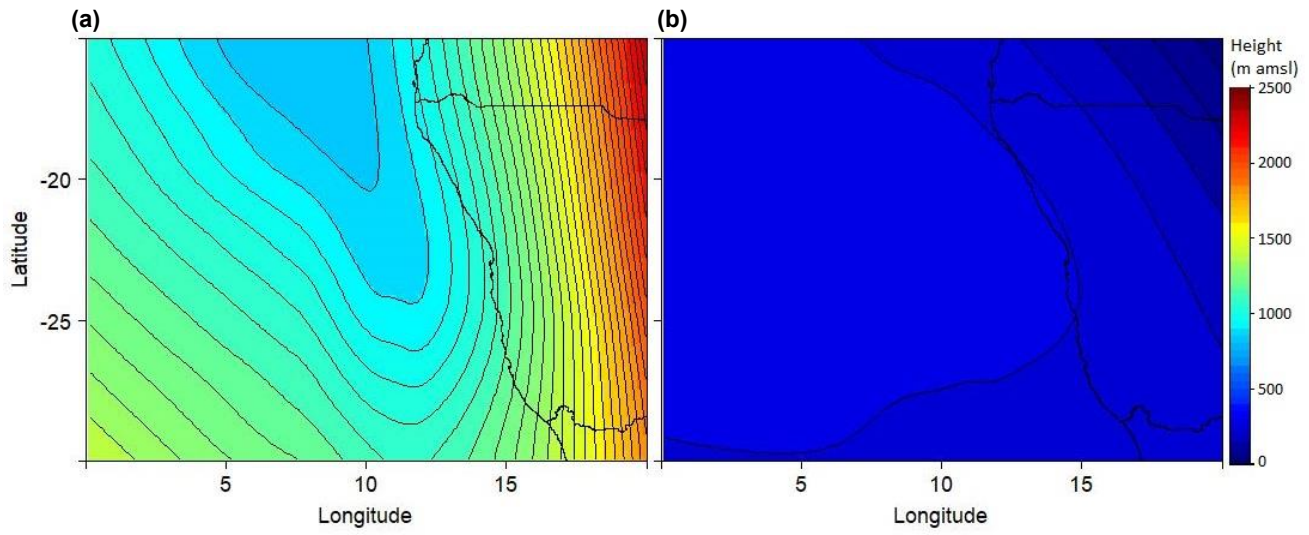


Figure S.5: The overall (a) mean and (b) standard deviation of the height of low-level temperature inversions over the area of interest. Polynomial smoothing was applied to the data.

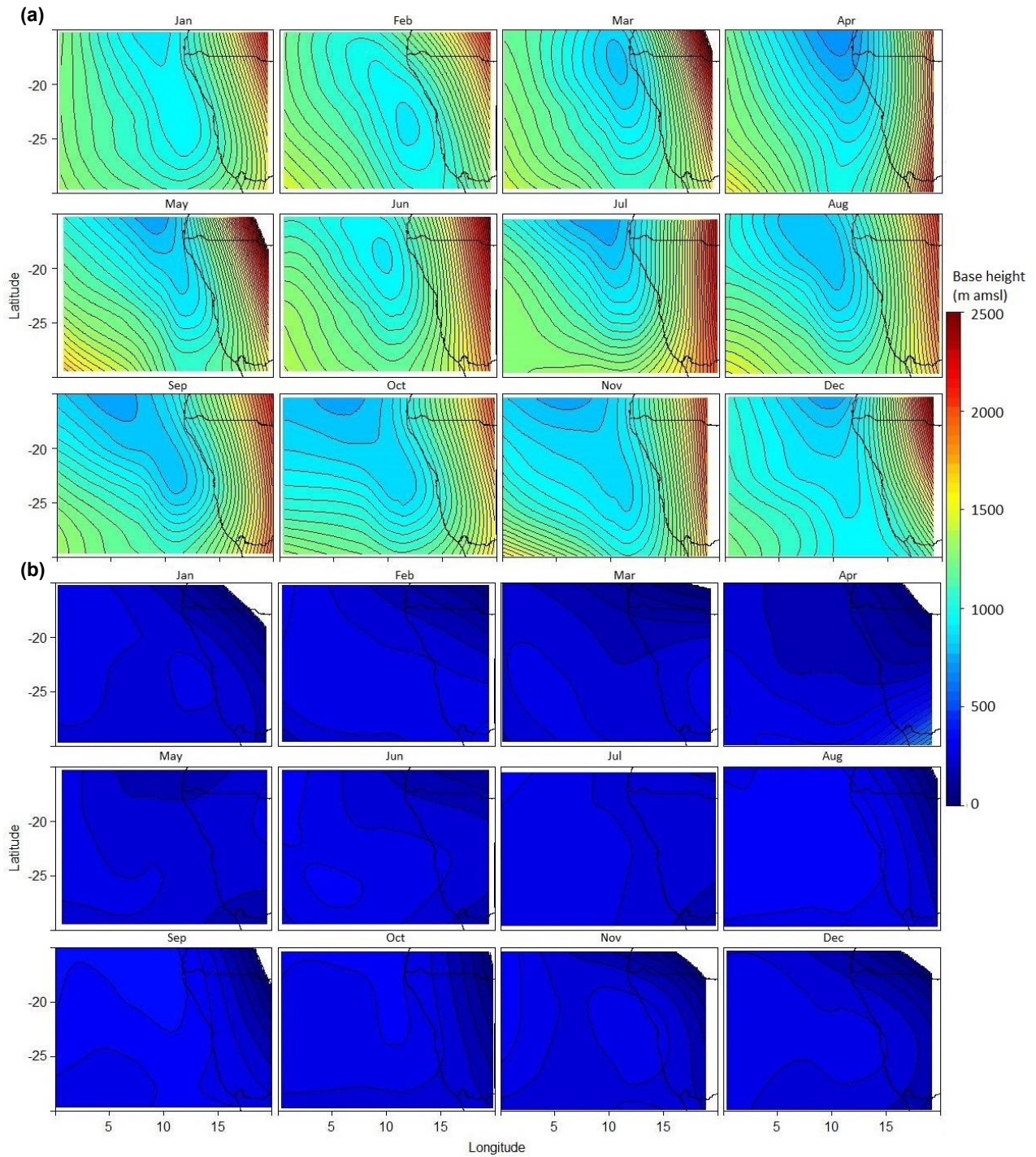


Figure S.6: The monthly (a) mean and (b) standard deviation of the low-level inversion base height over the area of interest. Polynomial smoothing was applied to the data.

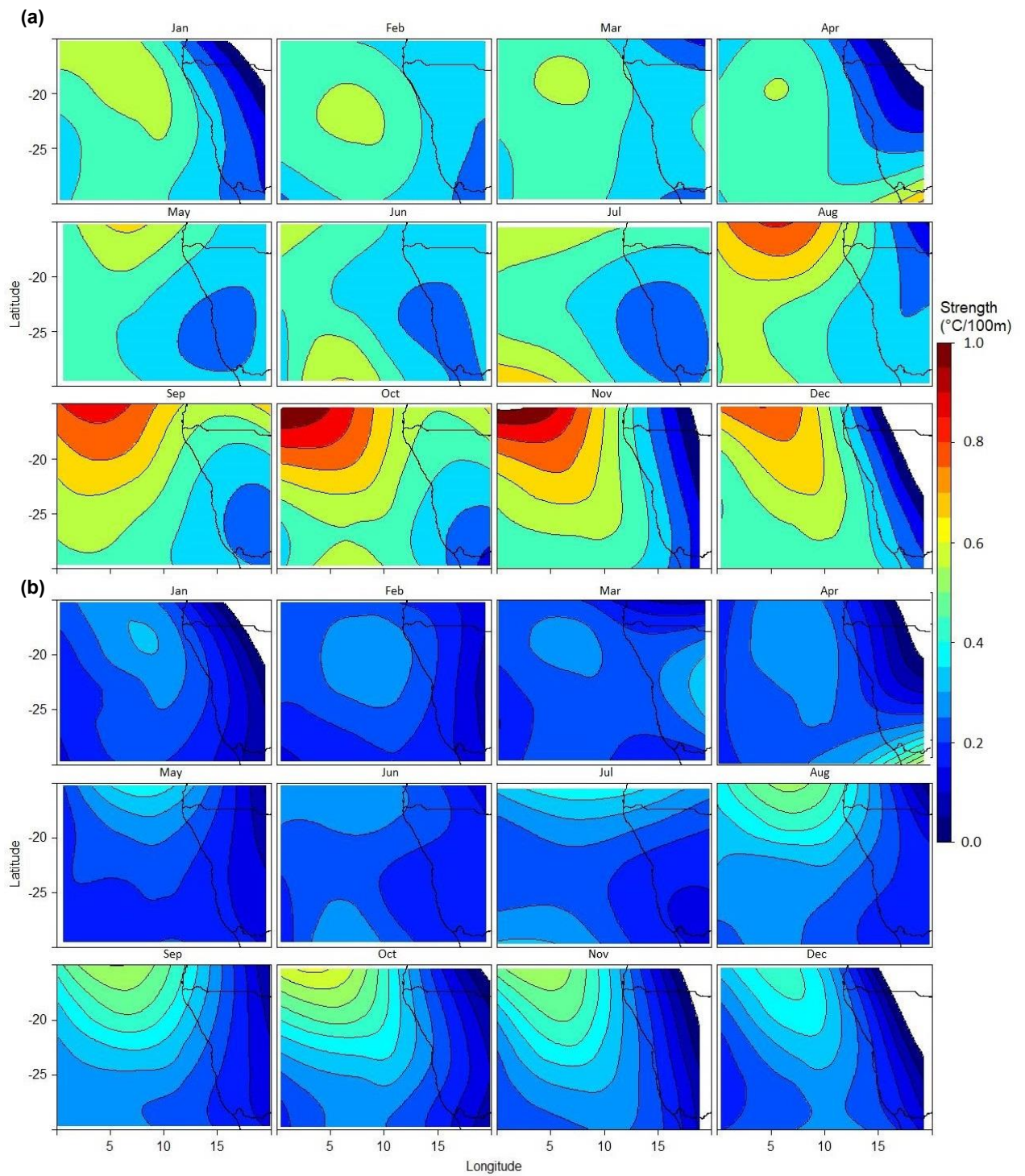


Figure S.7: The monthly (a) mean and (b) standard deviation of the low-level inversion strength over the area of interest. Polynomial smoothing was applied to the data.

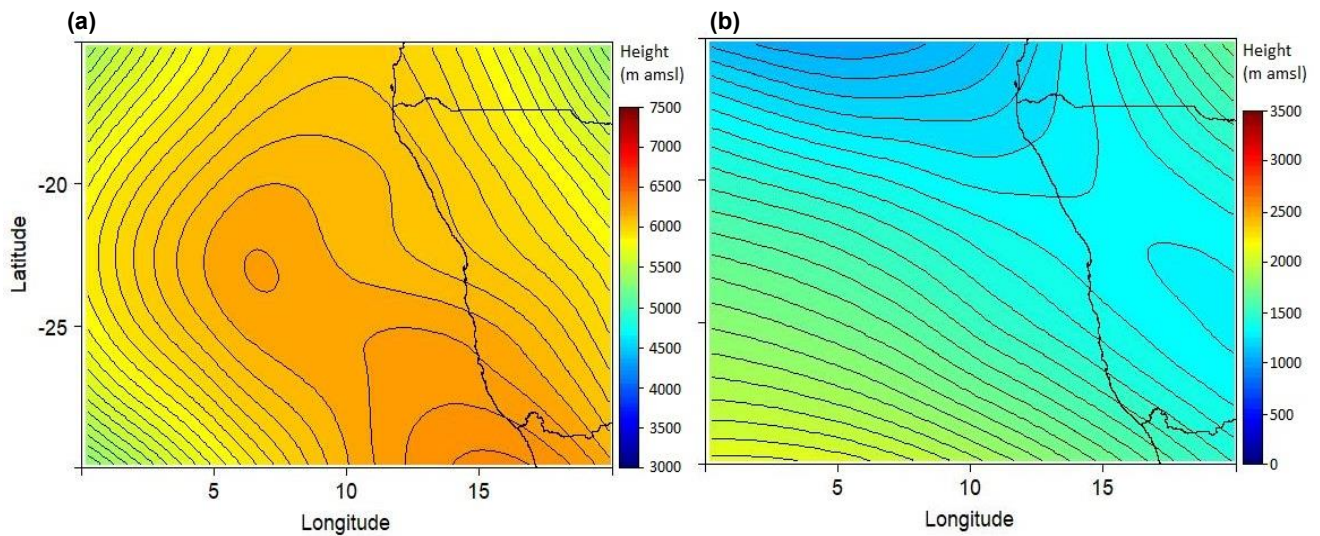


Figure S.8. The overall (a) mean and (b) standard deviation of the height of elevated temperature inversions over the area of interest. Polynomial smoothing was applied to the data.

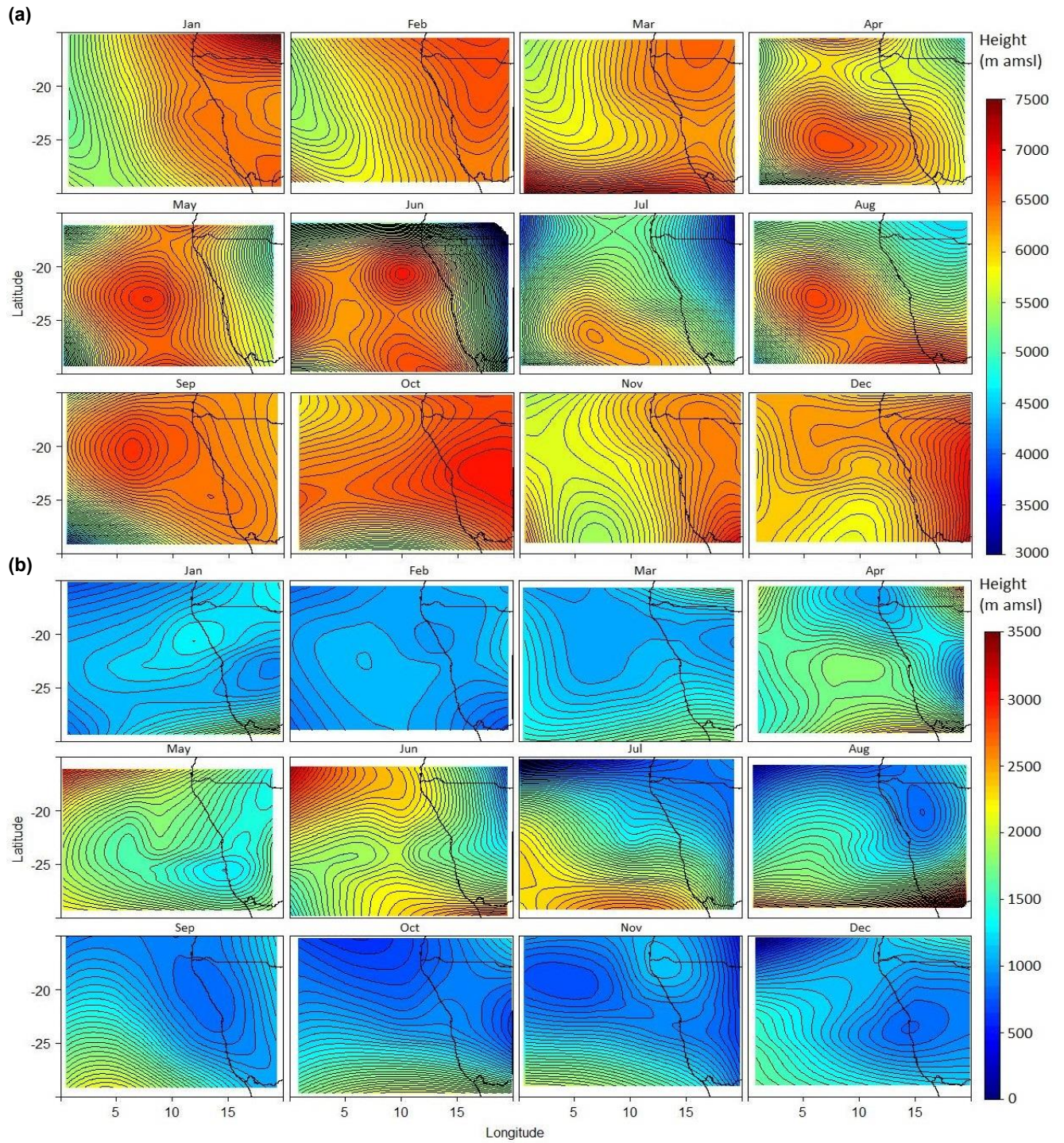


Figure S.9: The monthly (a) mean and (b) standard deviation of the elevated inversion base height over the area of interest. Polynomial smoothing was applied to the data.

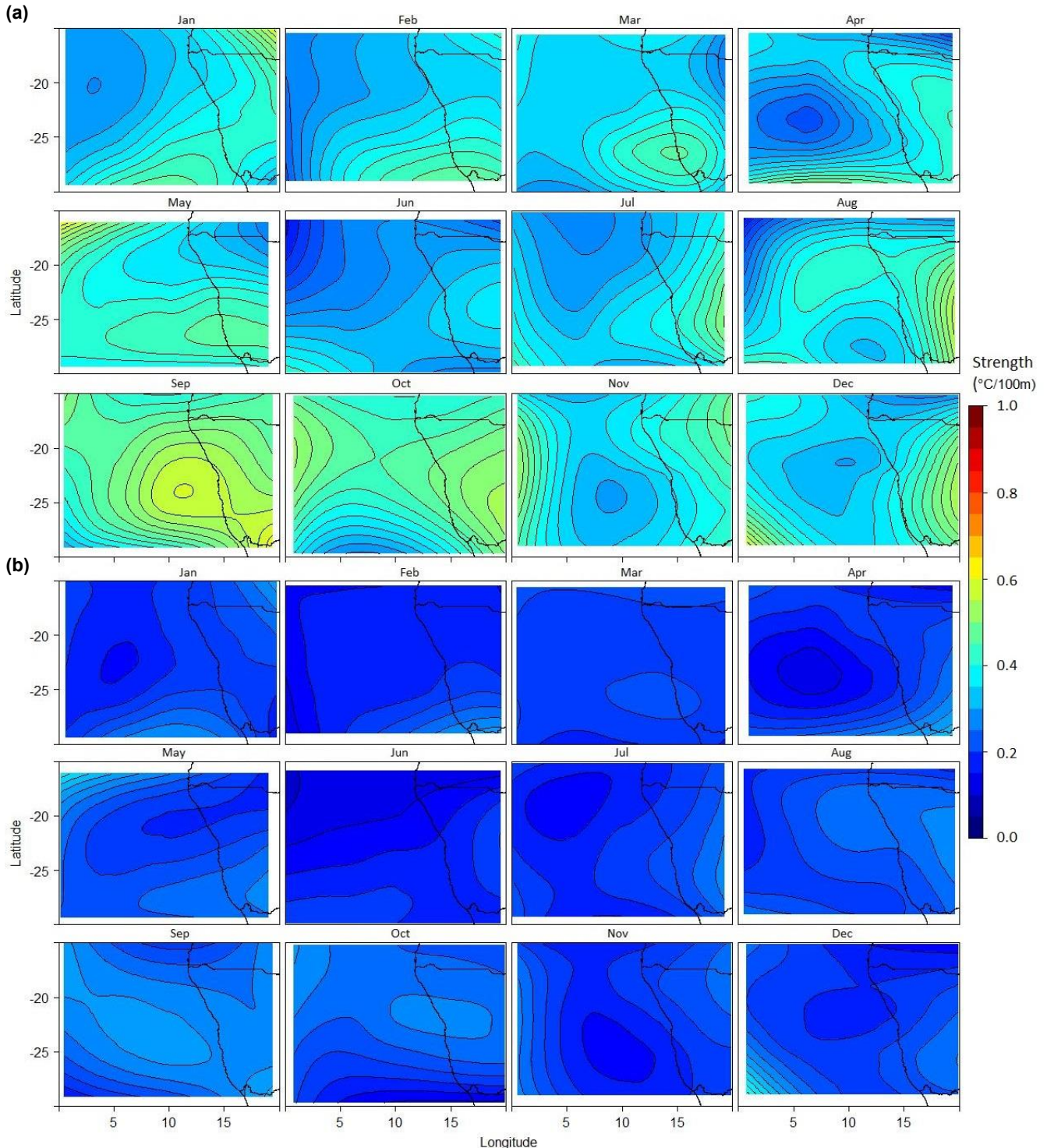


Figure S.10: The monthly (a) mean and (b) standard deviation of the elevated inversion strength over the area of interest. Polynomial smoothing was applied to the data.

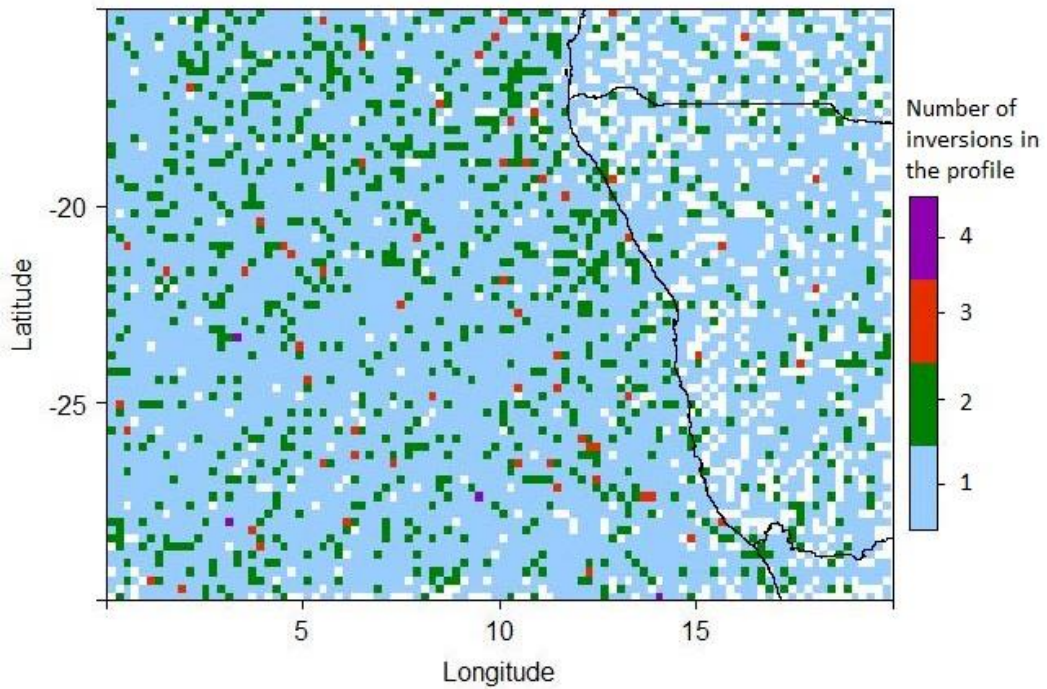


Figure S.11: A summary of the number of inversions measured in a single profile over the greater area of interest.

Table S.1: Monthly mean marine boundary layer height (m amsl) estimated by three different methods (described in section 4.2.) from radiosonde measurements made from Walvis Bay airport in 2015 at 9h and 10h UTC.

	Bulk Richardson number	Top of a surface-based inversion	Virtual potential temperature
Jan.	1059 ± 273	116 ± 10	316 ± 20
Feb.	1027 ± 195	109 ± 15	318 ± 17
Mar.	820 ± 198	131 ± 15	315 ± 17
Apr.	877 ± 610	126 ± 12	322 ± 23
May	688 ± 544	141 ± 1	322 ± 14
Jun.	1108 ± 976	138 ± 11	319 ± 18
Jul.	1009 ± 735	-	321 ± 17
Aug.	932 ± 369	100 ± 1	322 ± 19
Sept.	937 ± 317	132 ± 26	328 ± 26
Oct.	964 ± 177	116 ± 2	318 ± 19
Nov.	894 ± 228	122 ± 7	323 ± 24
Dec.	942 ± 218	131 ± 3	318 ± 19

Table S.2: Monthly mean height (m amsl) of the minimum gradient of refractivity calculated from co-located GPS-RO and radiosondes (limited to a minimum of 500 m amsl).

	GPS-RO	Radiosonde
Jan.	2170 ± 1170	1520 ± 880
Feb.	2090 ± 980	1220 ± 510
Mar.	2220 ± 1130	1790 ± 1020
Apr.	2860 ± 650	2100 ± 1130
May	2620 ± 990	2570 ± 1250
Jun.	1900 ± 940	2200 ± 770
Jul.	2800 ± 830	2050 ± 1060
Aug.	1180 ± 480	1910 ± 1150
Sept.	1320 ± 410	1240 ± 500
Oct.	670 ± 380	1160 ± 500
Nov.	2050 ± 930	1540 ± 870
Dec.	2240 ± 1050	1300 ± 620

Table S.3: Mean and standard deviation of the base heights (m amsl), base pressure (hPa), depths (m), strengths ($^{\circ}\text{C}/100 \text{ m}$) and strength throughout the depth ($^{\circ}\text{C}/\text{depth}$) of low-level inversions (0.5 – 2.5 km) identified in the COSMIC GPS-RO data in the 15° to 20°S , 20° to 25°S , and 25° to 30°S zonal bands over the region of interest, divided into oceanic, coastal and subcontinental regions. The data is summarised by time of day where N=noon (09h00 to 13h00 UTC), A=afternoon (13h00 to 17h00), and Ni=night (17h00 to 03h00). The frequency of measurements by time of day is also given.

	15° to 20°S			20° to 25°S			25° to 30°S			
	Ocean	Coast	Subcontinent	Ocean	Coast	Subcontinent	Ocean	Coast	Subcontinent	
Height (m amsl)	M.	980 ± 360	800 ± 300	1590 ± 270	1060 ± 410	920 ± 370	1740 ± 280	1180 ± 470	1130 ± 490	1550 ± 350
	N.	900 ± 310	730 ± 180	2270 ± 320	1020 ± 400	810 ± 330	2420 ± 100	1160 ± 470	1020 ± 440	2010 ± 200
	A.	930 ± 350	750 ± 240	2430 ± 60	1010 ± 400	770 ± 240	2320 ± 50	1120 ± 460	1100 ± 600	2140 ± 270
	Ni.	970 ± 350	850 ± 320	1630 ± 270	1050 ± 390	870 ± 340	1770 ± 320	1170 ± 460	1070 ± 480	1620 ± 370
Depth (m)	M.	400 ± 200	400 ± 300	200 ± 100	400 ± 200	400 ± 200	200 ± 200	400 ± 200	300 ± 200	300 ± 200
	N.	400 ± 200	400 ± 200	400 ± 100	400 ± 200	400 ± 300	400 ± 300	400 ± 200	300 ± 200	600 ± 1200
	A.	400 ± 200	400 ± 200	300 ± 300	400 ± 200	400 ± 300	400 ± 300	400 ± 200	300 ± 200	300 ± 200
	Ni.	400 ± 200	400 ± 200	200 ± 100	400 ± 300	400 ± 300	300 ± 600	400 ± 200	400 ± 200	300 ± 200
Strength ($^{\circ}\text{C}/100\text{m}$)	M.	0.58 ± 0.37	0.45 ± 0.28	0.38 ± 0.29	0.49 ± 0.34	0.36 ± 0.24	0.32 ± 0.2	0.44 ± 0.33	0.31 ± 0.21	0.32 ± 0.2
	N.	0.63 ± 0.38	0.49 ± 0.31	0.37 ± 0.14	0.5 ± 0.34	0.35 ± 0.21	0.26 ± 0.12	0.45 ± 0.34	0.28 ± 0.21	0.5 ± 0.72
	A.	0.61 ± 0.41	0.46 ± 0.29	0.46 ± 0.18	0.49 ± 0.35	0.35 ± 0.21	0.25 ± 0.06	0.45 ± 0.34	0.27 ± 0.17	0.22 ± 0.12
	Ni.	0.59 ± 0.38	0.44 ± 0.27	0.34 ± 0.19	0.47 ± 0.32	0.37 ± 0.22	0.43 ± 0.8	0.44 ± 0.32	0.32 ± 0.21	0.26 ± 0.18
Strength ($^{\circ}\text{C}/\text{depth}$)	M.	2.21 ± 2.22	1.64 ± 1.7	0.49 ± 0.56	1.91 ± 2.27	1.3 ± 1.33	0.78 ± 1.18	1.79 ± 2.43	0.95 ± 0.94	0.81 ± 0.83
	N.	2.35 ± 2.12	1.91 ± 1.79	1.7 ± 0.78	1.97 ± 2.21	1.47 ± 1.53	0.91 ± 1.1	1.93 ± 2.8	0.84 ± 0.87	10.77 ± 30.76
	A.	2.3 ± 2.26	1.55 ± 1.43	1.63 ± 1.77	2.04 ± 2.3	1.27 ± 1.15	0.85 ± 0.99	1.99 ± 2.83	0.75 ± 0.76	0.66 ± 0.72
	Ni.	2.18 ± 2.34	1.51 ± 1.46	0.41 ± 0.4	1.92 ± 2.11	1.53 ± 1.47	5.54 ± 32.21	1.79 ± 2.45	1.14 ± 1.09	0.77 ± 1.17
Number of inversions	M.	973	160	63	1472	247	63	1173	182	55
	N.	946	137	3	1423	152	8	1161	119	9
	A.	766	113	3	1074	125	4	881	129	16
	Ni.	926	151	28	1371	190	43	1150	175	43

Table S.4: Mean and standard deviation of the base heights (m amsl), base pressure (hPa), depths (m), strengths ($^{\circ}\text{C}/100\text{ m}$) and strength throughout the depth ($^{\circ}\text{C}/\text{depth}$) of elevated inversions (2.5 – 10 km) identified in the COSMIC GPS-RO data in the 15° to 20°S , 20° to 25°S , and 25° to 30°S zonal bands over the region of interest, divided into oceanic, coastal and subcontinental regions. The data is summarised by time of day where N=noon (09h00 to 13h00 UTC), A=afternoon (13h00 to 17h00), and Ni=night (17h00 to 03h00). The frequency of measurements by time of day is also given.

		15° to 20°S			20° to 25°S			25° to 30°S		
		Ocean	Coast	Subcontinent	Ocean	Coast	Subcontinent	Ocean	Coast	Subcontinent
Height (m agl)	M.	5860 ± 1450	6040 ± 1370	5440 ± 1590	6160 ± 1700	6080 ± 1260	6030 ± 1390	5810 ± 1960	6120 ± 1690	5870 ± 1570
	N.	5990 ± 1380	5870 ± 1430	5510 ± 1610	5910 ± 1700	6160 ± 1400	5970 ± 1420	6090 ± 1880	6220 ± 1850	6030 ± 1370
	A.	5990 ± 1390	6000 ± 1340	5670 ± 1570	6220 ± 1710	6100 ± 1590	5890 ± 1460	6340 ± 1900	6220 ± 1800	6260 ± 1370
	Ni.	6040 ± 1310	6160 ± 1190	6190 ± 1480	6400 ± 1670	6250 ± 1360	5990 ± 1430	6050 ± 1850	6450 ± 1770	6250 ± 1350
Depth (m)	M.	200 ± 200	200 ± 100	200 ± 200	200 ± 200	200 ± 100				
	N.	200 ± 300	200 ± 300	200 ± 200	200 ± 200	200 ± 300	200 ± 300	200 ± 200	200 ± 300	200 ± 300
	A.	200 ± 200	200 ± 200	200 ± 200	200 ± 300	200 ± 100	200 ± 200	200 ± 200	200 ± 100	200 ± 100
	Ni.	200 ± 200	200 ± 100	200 ± 200	200 ± 100					
Strength ($^{\circ}\text{C}/100\text{m}$)	M.	0.37 ± 0.24	0.41 ± 0.27	0.37 ± 0.25	0.35 ± 0.25	0.43 ± 0.3	0.43 ± 0.29	0.39 ± 0.35	0.47 ± 0.34	0.46 ± 0.29
	N.	0.37 ± 0.26	0.36 ± 0.3	0.33 ± 0.22	0.36 ± 0.25	0.43 ± 0.32	0.38 ± 0.27	0.4 ± 0.28	0.41 ± 0.3	0.46 ± 0.36
	A.	0.35 ± 0.27	0.31 ± 0.18	0.34 ± 0.27	0.36 ± 0.31	0.32 ± 0.19	0.42 ± 0.3	0.38 ± 0.39	0.36 ± 0.23	0.41 ± 0.26
	Ni.	0.36 ± 0.21	0.41 ± 0.42	0.41 ± 0.27	0.35 ± 0.24	0.42 ± 0.27	0.45 ± 0.32	0.37 ± 0.27	0.42 ± 0.26	0.46 ± 0.33
Strength ($^{\circ}\text{C}/\text{depth}$)	M.	0.69 ± 1.64	0.8 ± 1.88	0.77 ± 1.64	0.65 ± 1.87	0.84 ± 1.91	0.68 ± 1.08	0.8 ± 1.87	1.07 ± 2.23	0.78 ± 1.01
	N.	1.15 ± 4.28	1.13 ± 3.87	0.81 ± 2.29	0.77 ± 2.15	1.16 ± 3.14	1.05 ± 2.98	0.95 ± 2.32	1.28 ± 3.69	1.46 ± 6.5
	A.	0.65 ± 1.74	0.52 ± 1.01	0.68 ± 1.54	1.09 ± 6.4	0.41 ± 0.46	0.85 ± 1.13	0.67 ± 1.23	0.51 ± 0.63	0.66 ± 0.81
	Ni.	0.69 ± 1.81	1.04 ± 4.12	0.78 ± 1.33	0.61 ± 0.86	0.88 ± 3	1.06 ± 2.72	0.65 ± 1.14	0.79 ± 0.9	0.85 ± 1.27
Number of inversions	M.	276	124	273	323	189	241	282	120	100
	N.	214	117	219	267	150	178	280	101	67
	A.	180	81	141	202	87	126	231	100	56
	Ni.	217	150	297	300	171	233	263	112	89

